Journal of Polymers and the Environment (2019) 27:1488–1496
https://doi.org/10.1007/s10924-019-01447-6

ORIGINAL PAPER

Formulation of Green Particulate Composites from PLA and PBS Matrix and Wastes Deriving from the Coffee Production

Grazia Totaro[1] · Laura Sisti[1] · Maurizio Fiorini[1] · Isabella Lancellotti[2] · Fernanda N. Andreola[2] · Andrea Saccani[1]

Published online: 17 April 2019

Abstract

Particulate composites based on poly(lactic acid) and poly(butylene succinate) biopolymers have been formulated. Silver skin, the by-product derived from the roasting of coffee beans, has been used as a filler up to a 30 wt% of loading. The microstructure, crystallinity, thermal stability, mechanical properties and water absorption of the derived composites have been investigated. Data so far collected underline that a trade-off of the mechanical properties can be obtained by adding the filler, while the overall amount of crystallinity remains constant. Up to the highest filler content, moisture uptake follows a Fichian behaviour while the value of the contact angle is slightly increased by modification. Thus, silver skin, which actually is used for fuel or soil fertilization, finds here a different environmentally friendly valorization into the field of biocomposites.

Keywords PLA · PBS · Green composite · Agro-waste · Coffee production

Introduction

Circular economy is becoming an imperative goal of society in order to ensure further sustainable developments. Waste valorisation is a key aspect of this challenge. Agricultural wastes offer the advantage of being generally non-toxic and can consequently be recycled without any pre-treatment. Agro-wastes can be exploited to recover valuable chemicals. Antioxidant [1–4] are one of the main products that can be obtained. However, ad hoc chemical treatments are requested to recover substances from agro-wastes: this approach implies economical efforts and does not completely eliminate the problem of wastes. A different approach takes advantage on the use of agro-wastes as fillers to produce polymer matrix composites on account of their almost negligible cost. Although traditional oil-derived commodities, such as polyethylene, polypropylene or PVC [5–10] can be loaded by these fillers, higher environmental benefits can be obtained by using renewable polymers as a matrix. PLA is the most investigated among them [11]. Residuals of wine production [12], orange peel flour [13], lignin based fillers [14, 15], farm dairy effluents [16], almond shells [17] and nutshells [18] have been used as a dispersed second phase.

PBS is another renewable polyester gaining attention as a potential substitute for the traditional materials in packaging [19–24].

Coffee is one other important, widespread source of agro-wastes [25, 26]. It has been investigated in different forms either as a source of antioxidant and valuable chemicals [27–30] and as a filler in composites [31–36]. Silver skin is the integument surrounding the coffee beans and after the roasting process, it becomes a by-product. About one hundred kilograms of silver skin is produced out of five ton of roasted coffee. Some researchers have been made to promote its recycling [37, 38], but presently silver skin is just sent to damping. In the present study, the formulation of composites containing up to a 30 wt% of silver skin as a filler have been investigated exploiting PLA and PBS as matrixes. The most predictable use of these materials is in the packaging industry, which offers the opportunity of employing large amounts of wastes. At the same time, waste loading can lower the overall material price that is presently the limiting factor to the widespread diffusion of renewable polymers. So far, the mechanical properties, thermal stability and moisture

✉ Laura Sisti
laura.sisti@unibo.it

[1] Department of Civil, Chemical, Environmental and Materials Engineering, University of Bologna, Viale Terracini 28, 40128 Bologna, Italy

[2] Department of Engineering "Enzo Ferrari", University of Modena and Reggio Emilia, Via Vignolese 905, 41125 Modena, Italy

interaction of the composites have been investigated to assess materials reliability to this task.

Experimental

Materials

Commercial PLA (Ingeo™ Biopolymer 3100HP) with a density of 1.24 g/ml and a MFR of 24 g/10 min (210 °C, 2.16 kg) was obtained from NatureWorks. Commercial PBS (PBE003) with a density of 1.26 g/ml with a MFR of 4–6 g/10 min (190 °C, 2.16 kg) was obtained from NaturePlast.

The filler, silver skin (hereafter referred to as SSK), was kindly supplied by Cagliari spa (Modena, Italy). The morphology of the as received SSK is reported in Fig. 1. Before compounding, SSK was ball-milled for 20 min to obtain the final particle size distribution reported in Fig. 2 and the morphology shown in the same Figure. The milled waste has an almost equiaxed shape lacking the high l/d values typical of fibers reinforcement.

Filler Characterization

The total content of C, H, N and S was determined by combustion of the samples in an O_2 atmosphere using the Elemental Analyzer THERMOFISHER mod. FLASH 2000. The surface chemical composition of SSK was evaluated by ATR FT-IR over the wavenumber range 650–4000 cm^{-1} by accumulation of 32 scans at a resolution of 4 cm^{-1}, using a Perkin Elmer Spectrum One FT-IR spectrometer equipped with a Universal ATR sampling accessory.

The mineralogical analysis of the silver skin powder was carried out by using a conventional Bragg–Brentano powder diffractometer (PW3710, Phillips) with Ni-filtered Cu Kα radiation using brackett holder. The patterns have been recorded on the powdered sample (< 38 μm in size) in the 5–70° 2θ range (step size 0.02° and 1 s counting time for each step). The identification of crystalline phases was made under comparison with data on the JCPDS files.

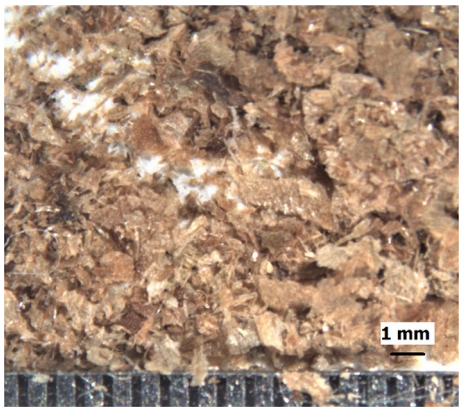

Fig. 1 Morphology of the as received SSK

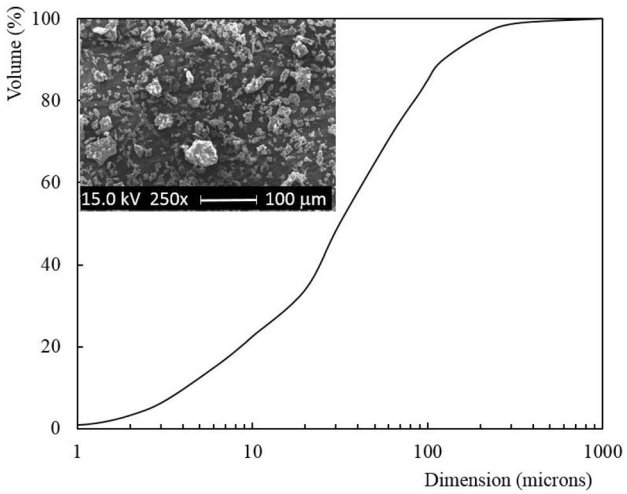

Fig. 2 Size distribution and morphology of ball-milled SSK

Composite Manufacturing

Braebender® batch mixer was used to mix PLA and PBS with SSK (10, 20 and 30 wt% respect to the polymer). Compounding was carried out at 190 °C (PLA) and 125 °C (PBS) respectively for 10 min at 60 rpm. Before compounding, all materials were treated for 12 h in vacuo at 60 °C to eliminate adsorbed moisture. The obtained materials were milled at low temperature. The samples prepared reported in Table 1 are named PBSXSSK, or PLAXSSK where X is 10, 20 or 30 wt%. Out of the derived powders, the following specimens were obtained: dog-bone samples (2 × 5 × 30 mm) to be submitted to tensile tests, discs with a 30 mm diameter and 1 mm thickness for contact angle and moisture absorption tests.

Table 1 Summary of the samples investigated

Matrix	Sample	SSK (wt%)
PLA	PLA	0
	PLA10SSK	10
	PLA20SSK	20
	PLA30SSK	30
PBS	PBS	0
	PBS10SSK	10
	PBS20SSK	20
	PBS30SSK	30

Tests and Procedures

Thermal stability of the materials was evaluated from the thermograms recorded from 50 to 800 °C in nitrogen flow (40 ml/min), scan rate 10 °C/min, by means of a Thermo Gravimetric PerkinElmer TGA4000.

The calorimetric analysis was carried out by means of a Perkin Elmer DSC6. Measurements were performed under nitrogen flow. To delete their previous thermal history, samples (about 10 mg) were first heated at 20 °C min^{-1} from 40 to 140 °C (PBS) or 220 °C (PLA), kept at the highest temperature for 2 min and then cooled to − 60 °C (PBS) or 0 °C (PLA) at 10 °C min^{-1}. After this thermal treatment, the samples were analyzed by heating from − 60 °C or 0 °C to 140 °C or 220 °C at 10 °C min^{-1} (2nd scan). During the cooling scan the crystallization temperature (T_c) and the enthalpy of crystallization (ΔH_c) were measured. During the 2nd scan the glass transition temperature (T_g), the melting temperature (T_m), the enthalpy of melting (ΔH_m), the cold crystallization temperature (T_{cc}) and its enthalpy (ΔH_{cc}) were measured. The degree of crystallinity (X_c) of the composites was calculated according to Eq. (1):

$$X_c(\%) = \frac{\Delta H_m - \Delta H_{cc}}{\Delta H_m^0}\frac{100}{w} \quad (1)$$

where $\left(\Delta H_m^0\right)$ is the enthalpy of 100% crystalline PLA (91.0 J/g) [39] or PBS (200.0 J/g) [40] and w is the weigth fraction of PLA or PBS in the composites.

Tensile tests were performed by an INSTRON 5966 series apparatus equipped with a 10kN load cell (test speed 5 mm/min, room temperature 19 ± 1 °C and 70 ± 10% R.H.) on five samples for each composition. The value of the Young modulus was obtained from the stress/strain curve without the use of extensometer, thus providing a lower value than that usually reported for PLA and PBS.

SEM analysis (FEI, XL20 microscope, secondary electrons detector) was carried out on the waste powders or on the unperturbed fracture surfaces of samples submitted to the tensile tests, after aluminium sputtering by means of an EMITECH mod. K550 equipment.

Water absorption has been measured on three disks for each composition. Samples were previously dried in vacuo at 60 °C for 24 h, to determine the initial dry weight; afterwards, they were stored at 98 ± 1% R.H. and 25 ± 1 °C and the weight was determined at scheduled times.

The water contact angles were measured using a drop shape analyser (DSA30S- Kruss). For every measurement point, the average value of contact angles measured on five locations on the sample was taken.

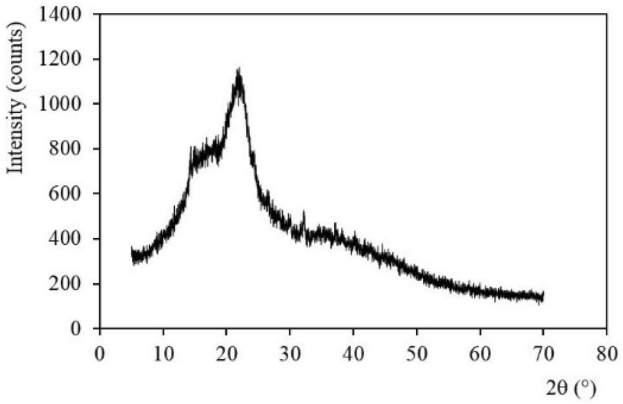

Fig. 3 X-ray analysis of SSK

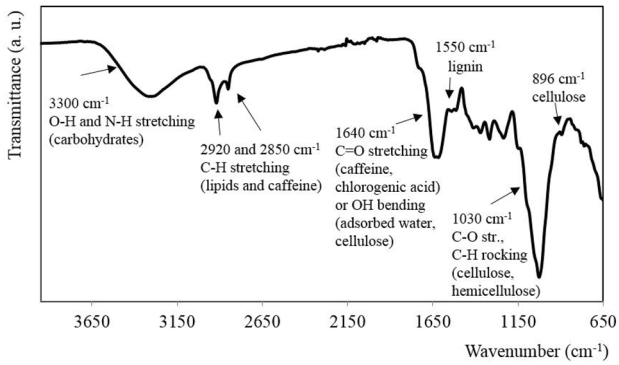

Fig. 4 FT-IR spectrum of SSK

Results and Discussion

Silver Skin Characterization

The elemental analysis of SSK can be summarised as it follows: N% 3.24; C% 44.07; H% 5.81; S% 0.00, ashes 9.32 wt% (550 °C after 4 h). Compared to the composition of other wastes deriving from the production of soluble coffee [25], SSK shows a higher amount of nitrogen and lower amounts of carbon and hydrogen. Data are quite similar to those of others SSK [37].

Figure 3 reports the X-ray analysis of the waste. The major crystalline peak occurs at 2θ = 23°, which represents the cellulose crystallographic plane (002 Brag Brentano) [41] while the remaining waste shows an amorphous character as underlined by the shape of the diffractogram at low 2θ values.

ATR FT-IR spectrum of SSK (Fig. 4) shows the characteristic absorption bands of lignocellulosic materials, mainly consistent in polysaccharides (cellulose, hemicellulose), lignin, proteins, fats and minerals. The broad band

around 3300 cm^{-1} is due to OH and NH stretching. Asymmetric and symmetric CH stretching are visible at 2920 and 2850 cm^{-1}. The latter band is reported in many caffeinated beverages and is usually associated to the methyl group in caffeine, while the first band is reported to be related to lipids [37]. The presence of caffeine is confirmed by the carbonyl stretching at 1640 cm^{-1}. Such band is also associated to chlorogenic acid [42] or adsorbed water [43]. The intense band at 1030 cm^{-1} is due to C–O stretching and CH rocking vibrations from polysaccharides. Those findings are in agreement with literature [37, 42, 43].

Concerning the thermal properties of SSK, Fig. 5 shows the TGA profile and the corresponding derivative curve. A 5 wt% loss takes place at low temperature (< 180 °C) due to water removal. The main decrease (about 50 wt%) takes place in SSK from 220 to 370 °C. This corresponds to the overlapping of two decomposition peaks, the lower referred to the decomposition of hemicellulose and the higher to cellulose [44].

This confirms data obtained from FT-IR and X-ray results. The remaining material, about 30 wt% of the whole amount, is partially made of lignin as witnessed by the small peak at 450 °C, which can be associated to partial decomposition of lignin and proteins. No further loss takes place up to the highest investigated temperature.

Composite Characterization

TGA curves of composites containing SSK from 10 to 30 wt% prepared using commercial PLA and PBS are reported in Fig. 6, while the thermal data are summarized in Table 1. As can be seen both PLA (Fig. 6a) and PBS (Fig. 6b) composites up to about 200 °C show the same behaviour as the one of the plain matrix. The curves, as well as the T_{onset} data, highlight that all composites present lower thermal stability as a function of filler loading: PLA and PBS matrix, having higher thermal stability respect to SSK, play a dominant role

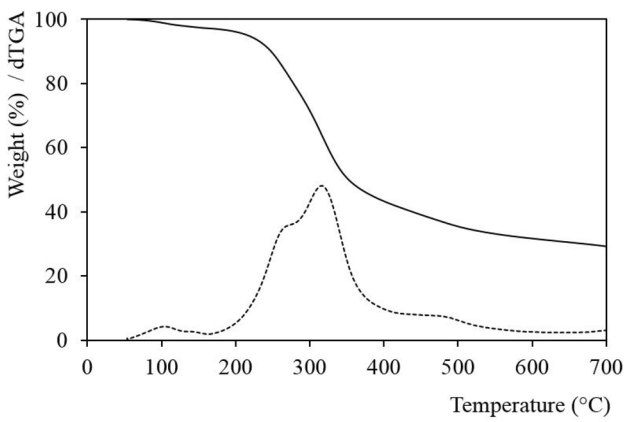

Fig. 5 TGA and dTGA profiles of SSK

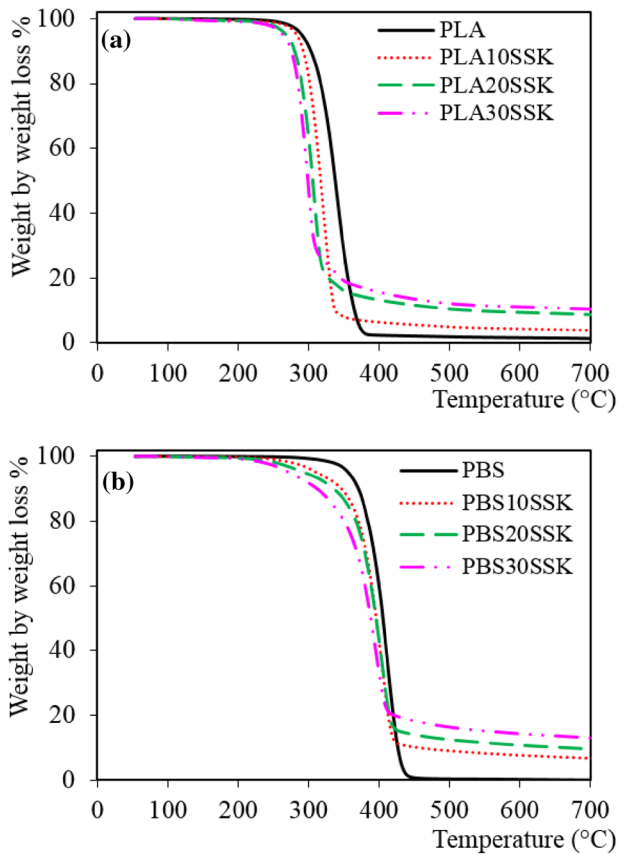

Fig. 6 TGA profiles of **a** PLA and its SSK composites and **b** PBS and its SSK composites

in thermal behaviour. The decrease can be due to two main reasons: the metals present in SSK, which can catalyse the degradation of the matrix as underlined in other researches [37, 45], and the moisture released by the filler, which can induce hydrolysis of the ester groups. This behaviour is more marked in PLA series probably because PLA is more sensitive to temperature and hydrolysis respect to PBS.

The results of DSC analysis are summarized in Table 2. The values of enthalpy have been referred to the amount of matrix present in the different composites.

For PLA, the main difference is found on the values of T_c that are at least 5 degrees below that of the plain matrix. The amount of crystallized polymer is also slightly decreased, thus indicating that the filler hinders the growth of the polymeric crystals and inhibits crystallization. This trend is not confirmed for the 30 wt% composition, in fact in this case the thermal data are closed to the one of the neat polymer. During the subsequent heating treatment, as also reported in literature [46], the polymer matrix is able to recrystallize (T_{cc}) at high temperature and then melts at around 175 °C. The presence of the cold crystallization is caused by a primary nucleation occurring above its T_g, when polymer

Table 2 Thermal characterization of the investigated materials

Sample	TGA	DSC							
		Cooling scan		2nd heating scan					
	T_{onset} (°C)	T_c (°C)	ΔH_c (J/g)	T_g (°C)	T_{cc} (°C)	ΔH_{cc} (J/g)	T_m (°C)	ΔH_m (J/g)	X (%)
PLA	315	102	32	61	101	7.5	176	43	39
PLA10SSK	296	95	21	58	94	7.9	174	42	42
PLA20SSK	287	96	24	58	92	2.6	173	44	57
PLA30SSK	282	97	33	57	89	0.6	170	46	71
PBS	381	84	67	−33	/	/	115	60	30
PBS10SSK	371	84	67	−32	/	/	114	61	34
PBS20SSK	366	82	68	−31	/	/	115	64	40
PBS30SSK	357	81	63	−34	/	/	114	63	45

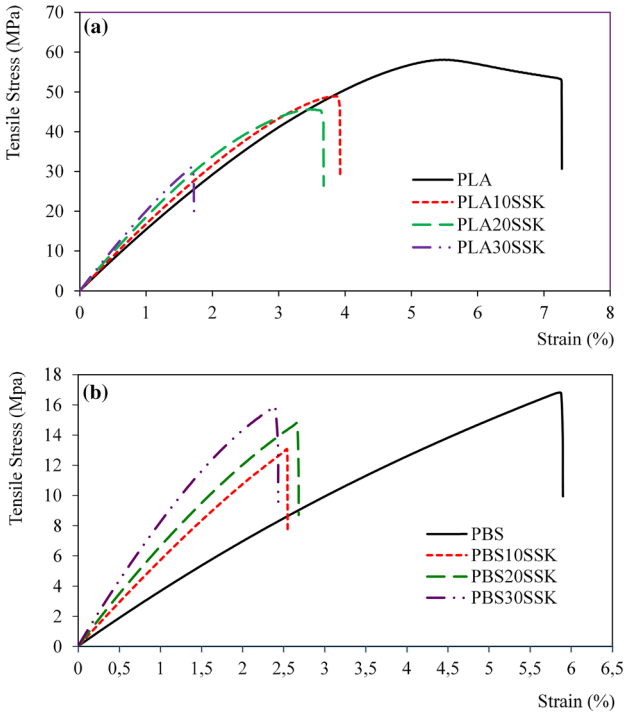

Fig. 7 Stress–strain curves from tensile tests of **a** PLA and its SSK composites and **b** PBS and its SSK composites

chains become flexible and achieve an ordered state via an exothermic process. The addition of SSK in general seems to decrease this phenomenon in particular for the 30 wt% composition. PBS instead crystallizes at 84 °C and melts at 115 °C. The composites do not show any significant difference respect to the homopolymer: all parameters (T_c, ΔH_c, T_m, ΔH_m) are quite similar and unaffected by the presence of the filler. Moreover, for both the polymer series, the addition of SSK determines an increase of the degree of crystallinity as already reported by Sarasini et al. [37].

With regards to the tensile properties Fig. 7 shows the typical stress–strain curves while Table 3 summarizes the

Table 3 Mechanical properties of PLA and PBS and their composites

	E (MPa)	σ_{max} (MPa)	ε_b (%)
PLA	1615 ± 11	59.2 ± 0.8	7.1 ± 1.5
PLA10SSK	1759 ± 3	47.2 ± 1.5	3.7 ± 0.2
PLA20SSK	1971 ± 25	45.9 ± 0.7	3.8 ± 0.4
PLA30SSK	2146 ± 10	29.1 ± 1.4	1.5 ± 0.1
PBS	375 ± 3	16.1 ± 0.9	5.6 ± 0.4
PBS10SSK	590 ± 5	13.0 ± 0.2	2.5 ± 0.1
PBS20SSK	699 ± 9	15.2 ± 0.9	2.8 ± 0.2
PBS30SSK	886 ± 9	16.1 ± 0.3	2.4 ± 0.1

corresponding mechanical properties (i.e. strength, modulus and deformation at break) for PLA and PBS composites. For both polymers, the addition of SSK increases the value of the elastic modulus. The increase is particularly strong in the case of PBS (+ 130% at 30 wt% of filler) but it is also remarkable in PLA (+ 30% at 30 wt% of filler). This can be considered as evidence of an efficient dispersion and wettability of the filler in the relative matrix. In both polymers, the deformation at break decreases as the amount of filler increases. This behavior has already been found in other composites where thermoplastic matrix has been modified by the addition of natural fibres [47–50]. As to what concerns tensile strength the effect is different in the two polymers. In PBS values are almost unaffected by the addition of SSK. In PLA based materials tensile strength decreases as the amount of filler increases particularly at the highest concentration. Different effects may contribute, in this case, to the frequently observed decrease in the tensile strength of filled thermoplastic matrix. First of all, degradation reactions taking place during compounding [51], leading to a decrease in PLA molecular weight accelerated by the presence of metal ions in SSK and then the slight hindering effect of the filler on crystalline phase development in the samples, as observed in DSC measurements. These processes are not observed in PBS composites due to the lower compounding

temperature (125 °C compared to the 190 °C of PLA). In the present research, it was not possible to determine the mechanical properties (i.e. tensile strength, elastic modulus) of the filler (SSK) and this hinders the possibility to perform detailed theorical analysis of the mechanical properties of the composites.

Figure 8 shows the fracture surfaces of PLA composites disclosing the composites microstructure, while Fig. 9 shows the fracture surfaces of PBS composites. No evidence of not homogeneous dispersion of the filler is observed even at the highest amounts in both composites. Filler addition creates a rougher surface than that of the plain polymers. However, no enhanced yielding is detected, as found for other organic fillers used to formulate PLA composites [12], in agreement with the decrease of the deformation at break reported in Table 2.

The values of contact angle are reported in Fig. 10, as a function of the waste amount. An increase is found in both materials as the amount of SSK increases, but it is more pronounced in PLA series. However, the data are associated to standard deviation values rather large, indicating a certain lack of homogeneity of the surface.

Water absorption is shown in Figs. 11a PLA and Fig. 11b PBS reported as a function of the squared root of time (hours).

SSK progressively increases the overall amount of absorbed water. The absorption trend is however asymptotic and the process still follows, even at the highest SSK content, Fickian behaviour. On account of the drastic conditions of humidity applied during the tests and on the limited increase on water uptake, all composites can be still considered reliable in packaging applications.

Conclusions

The main conclusions from the experimental work can thus be summarised:

– It is feasible to produce composite materials by adding up to a 30 wt% of silver skin to PLA and PBS polymers.

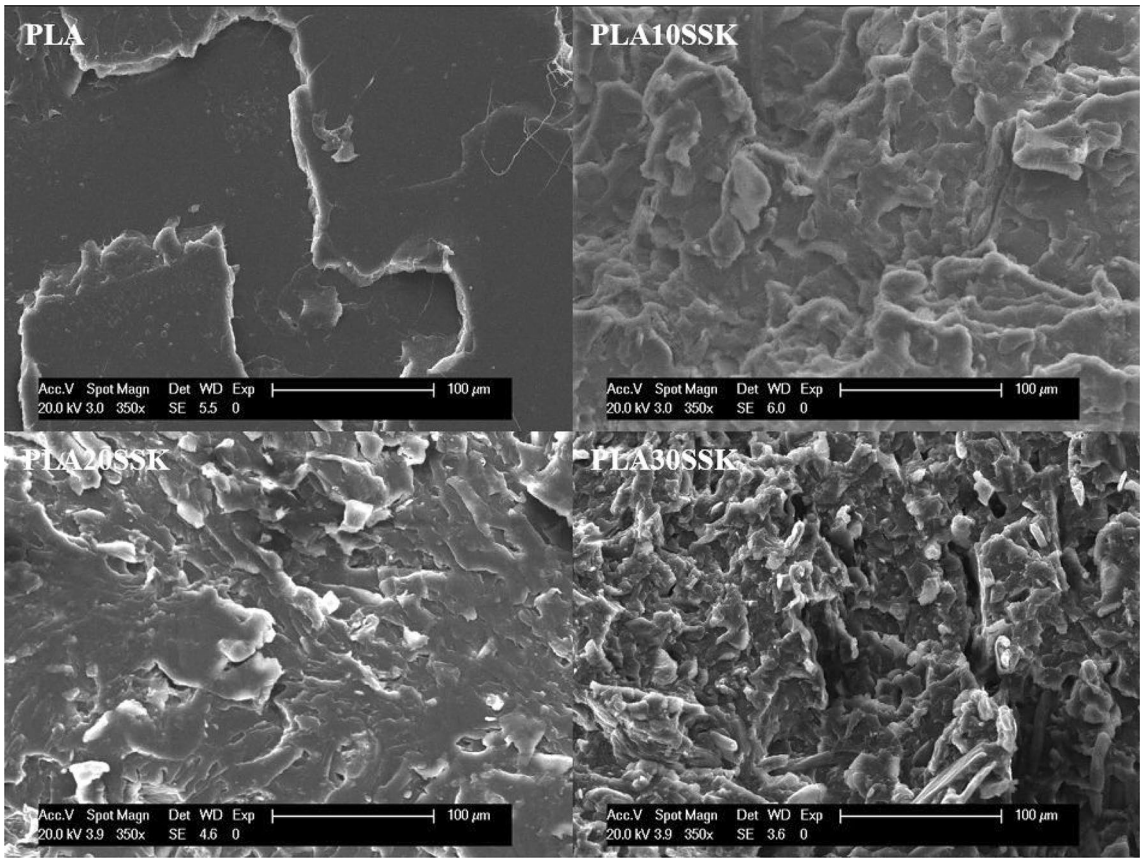

Fig. 8 Fracture surfaces of PLA based materials

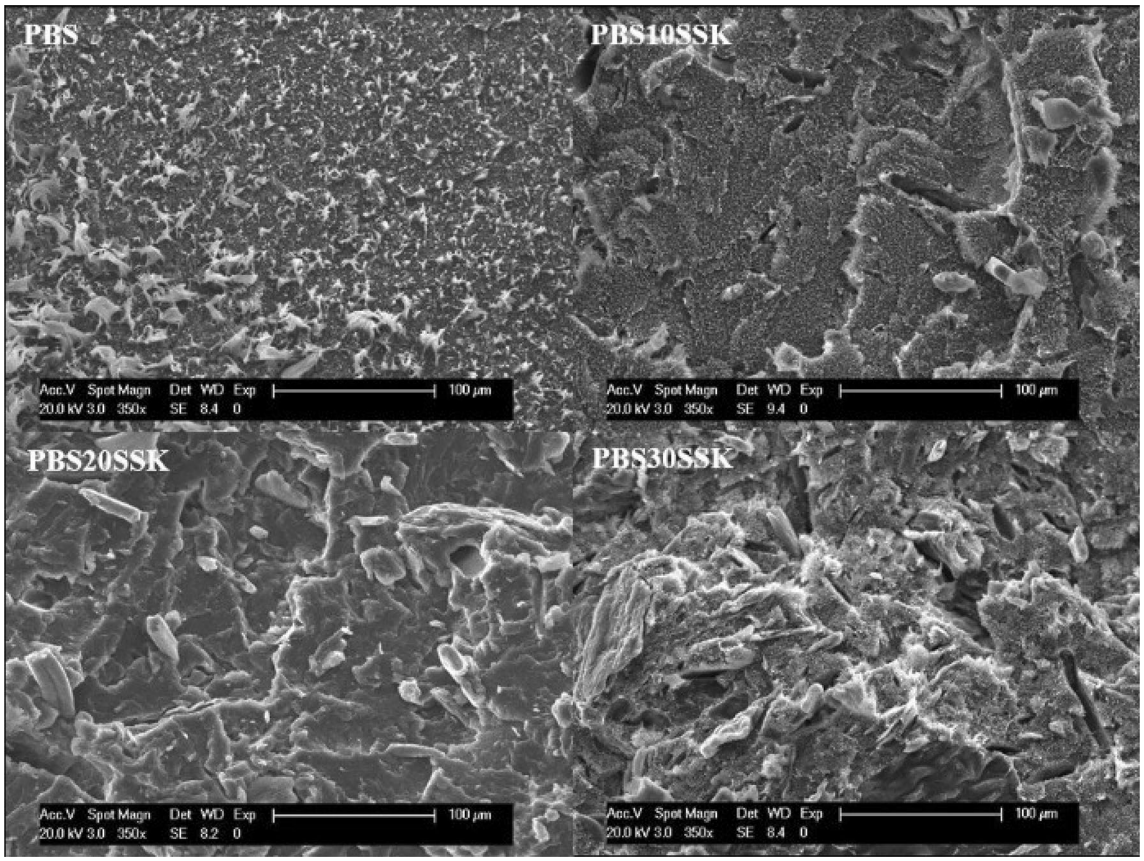

Fig. 9 Fracture surfaces of PBS based materials

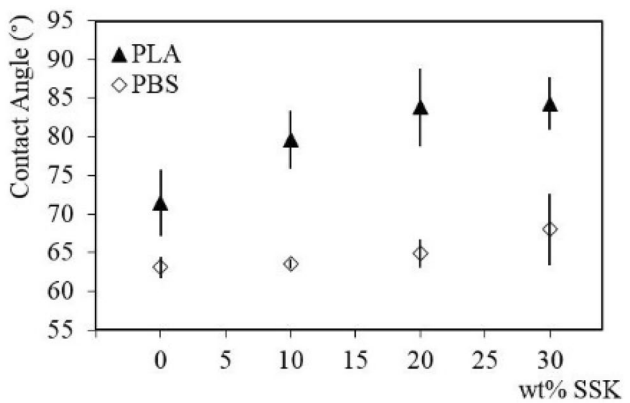

Fig. 10 Contact angle versus SSK content for the investigated composites

– This addition is particularly positive in PBS, where a large increase in the Young modulus is obtained, without decreasing the tensile strength of the materials. Moreover, the crystallization kinetic of the compounds is unaltered even at the highest silver skin content.
– In PLA a trade off concerning the mechanical properties can be obtained since the value of the Young modulus is increased while the tensile strength is progressively reduced on increasing the filler amount. Crystallization is only slightly hindered by the presence of silver skin.
– These differences can derive from the higher compounding temperature necessary in PLA composites that can lead to a partial decomposition of the filler affecting PLA performances.
– This approach has a high potential as to what concerns the diffusion of two of the most promising renewable polymers in packaging by both reducing the amount of matrix, that is presently more expensive than oil derived materials, and avoiding damping of silver skin.

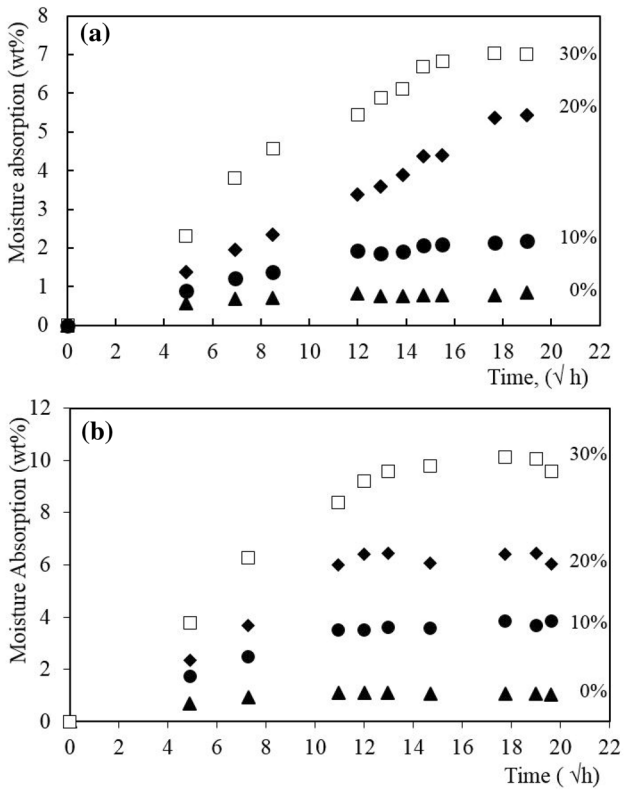

Fig. 11 Moisture absorption in **a** PLA and its composites and **b** PBS and its composites

Acknowledgements This research did not receive any specific grant from funding agencies in the public, commercial, or not-for-profit sectors. Thanks are due to Cagliari spa (Modena, Italy) for supplying silver skins.

References

1. Koutrotsios G, Kalogeropoulos N, Kaliora AC (2018) J Agric Food Chem 66(24):5971
2. Haas ID, Toaldo IM, Burin VM, Bordignon-Luiz MT (2018) Ind Crops Prod 112:593
3. Pinela J, Prieto MA, Barreiro MF (2017) Innovative Food Sci Emerg Technol 41:160
4. Iyer KA, Zhang L, Torkelson JM (2016) ACS Sustain Chem Eng 4:881
5. Kaya N, Atagur M, Akyu O, Seki Y, Sarikanat M, Sutcu M, Seydibeyoglu MO, Sever M (2018) Composites Part B 150:277
6. Lanjewar SR, Bari PS, Hansora DP (2018) Sci Eng Comp Mater 25:373
7. Mousa A, Heinrich G, Gohs U, Hassler R (2009) Polym Plast Technol Eng 4:1030
8. Mishra S, Verma J (2006) J Appl Polym Sci 101:2530
9. Mishra S, Naik JB (2005) Polym Plast Technol Eng 44:511
10. Chun KS, Yeng CM, Hussiensyah S (2018) Polym Comp 39:2441
11. Murariu M, Dubois P (2016) Adv Drug Delivery Rev 107:17
12. Saccani A, Sisti L, Manzi S, Fiorini M (2019) Polym Comp 40:1378
13. Quiles-Carrillo L, Montanes N, Lagaron MJ (2018) Polym Int 67:1341
14. Spiridon I, Leluk K, Resmerita AM, Darie RN (2015) Composites Part B 69:342
15. Liao H, Wu C (2012) J Polym Eng 32:435
16. Le Guen M, Thoury-Monbrun V, Castellano Rolda JM, Hill SJ (2017) J Polym Environ 25:419
17. Essabira H, Bensalah MO, Rodrigue D, Bouhfid R, Qaiss A (2016) Carbohydr Polym 143:70
18. Quiles-Carrillo L, Montanes N, Garcia-Garcia D (2018) Composites Part B 147:76
19. Frollini E, Bartolucci N, Sisti L, Celli A (2015) Polym Test 45:168
20. Sisti L, Totaro G, Vannini M, Fabbri P, Kalia S, Zatta A, Celli A (2016) Ind Crops Prod 81:56
21. Sisti L, Totaro G, Marchese P (2016) In: Kalia S, Averous L (eds) Biodegradable and biobased polymers for environmental and biomedical application. Wiley, Beverly, p 225
22. Sisti L, Kalia S, Totaro G, Vannini M, Negroni A, Zanaroli G, Celli A (2018) J Environ Chem Eng 6(4):4452
23. Totaro G, Sisti L, Vannini M, Marchese P, Tassoni A, Lenucci MS, Lamborghini M, Kalia S, Celli A (2018) Composites Part B 139:195
24. Thakur K, Kalia S, Kaith BS, Pathania D, Kumar A, Thakur P, Knittel CE, Schauer CL, Totaro G (2016) J Environ Chem Eng 4:1743
25. Pujol D, Liu C, Gominho J, Olivella MA, Fiol N, Villaescusa I, Pereira H (2013) Ind Crops Prod 50:423
26. Esquivel P, Jiménez VM (2012) Food Res Int 46:488
27. Regazzoni L, Saligari F, Marinello C (2016) J Funct Foods 20:472
28. Murthy M, Pushpa S, Naidu M (2012) Food Bioprocess Technol 5:897
29. Janissen B, Huynh T (2018) Resour Conserv Recycl 128:110
30. Pushpa S, Murthy M, Naidu M (2012) Resour Conserv Recycl 66:45
31. Baek B, Park J, Lee B, Kim HJ (2013) J Polym Environ 21:702
32. Wu C (2015) Polym Degrad Stab 121:51
33. Cacciotti I, Mori S, Cherubini V, Nanni F (2018) Int J Biol Macromol 112:567
34. Reis KC, Pereira L, Melo NIC, Marconcini A, Trugilho JM, Tonoli PF (2015) Mater Res 18(3):546
35. Murthy PS, Naidu MM (2012) Resour Conserv Recycl 66:45
36. Oliveira M, Mota C, Abreu AS, Nobrega JM (2015) J Polym Eng 35:401
37. Sarasini F, Tirillo J, Zuorro A, Maffei G, Lavecchia R, Puglia D, Dominici F, Luzi F, Valente T, Torre L (2018) Ind Crops Prod 118:311
38. Sung SH, Chang Y, Han J (2017) Carbohydr Polym 169:495
39. Pyda M, Bopp RC, Wunderlich B (2004) J Chem Thermodyn 36:731
40. Liang ZC, Pan PJ, Zhu B, Dong T, Inoue Y (2010) J Appl Pol Sci 115:3559
41. Imane K, Hamid S (2018) Ind Crops Prod 124:787
42. Ballesteros LF, Teixeira JA, Mussatto SI (2014) Food Bioprocess Technol 7:3493
43. Alghooneh A, Amini AM, Behrouzian F, Razav SMA (2017) Int J Food Prop 20:2830
44. Azwa ZN, Yousif BF, Manalo AC, Karunasena W (2013) Mater Des 47:424
45. Moustafa H, Guizani C, Dupont C, Martin V, Jeguirim M, Dufresne A (2017) ACS Sustain Chem Eng 5:1906
46. Sisti L, Belcari J, Mazzocchetti L, Totaro G, Vannini M, Giorgini L, Zucchelli A, Celli A (2016) Polym Test 50:283
47. Jiang N, Yu T, Li Y (2018) J Polym Evinron 26:3176
48. Wan Lu, Shuai Zhou, Yanhua Zhang (2019) Int J Biol Macromol 125:1093
49. Araújo RS, Marques MFV, de Oliveira PF, Rezende CC (2018) J Polym Environ 26:3785

50. Loureiro NC, Esteves JL, Viana JC, Ghosh S (2014) Composites Part B 60:603
51. Khanlou HM, Woodfield P, Summerscales J, Francucci G, King B, Talebian S, Foroughi G, Hall W (2018) Measurement 116:367